# A computational model for domain structure evolution of nematic liquid crystal elastomers

Hongbo Wang [1] and William S. Oates [2]

Florida Center for Advanced Aero-Propulsion–FCAAP[1,2]
Department of Mechanical Engineering[1,2]
Florida A&M/Florida State University
Tallahassee, FL 32310-6046

## Abstract

Liquid crystal elastomers combine both liquid crystals and polymers, which gives rise to many fascinating properties, such as unparalleled elastic anisotropy, photo-mechanics and flexoelectric behavior. The potential applications for these materials widely range from wings for micro-air vehicles to reversible adhesion skins for mobile climbing robots. However, significant challenges remain to understand the rich range of microstructure evolution exibited by these materials. This paper presents a model for domain structure evolution within the Ginzburg-Landau framework. The free energy consists of two parts: the distortion energy introduced by Ericksen [1] and a Landau energy. The finite element method has been implemented to solve the governing equations developed. Numerical examples are given to demonstrate the microstructure evolution.

**Keywords:** liquid crystal elastomer, domain structure, finite element

## 1. Introduction

Liquid crystals are fascinating materials that exhibit a number of liquid and solid phase characteristics. These materials flow like a fluid, but can also have long range crystal order like a solid. These interesting material properties have motivated materials scientists and chemist to formulate synthesis procedures that lead to multi-functional elastomers doped with liquid crystals [2–4]. This is achieved due to long-range liquid crystal order and field-coupled characteristics which can provide unparalleled elastic anisotropy [2, 5], electrostriction [6, 7], flexoelectricity [8], photo-mechanical coupling [9–11], and shape memory properties [12].

One of the main challenges in exploiting liquid crystal materials in elastomers is due to understanding complex interactions between the liquid crystal mesogen units (i.e., liquid crystal forming molecules) and the elastomer network. This problem is not new and has been extensively researched [13–21]. However, many questions remain on understanding the underlying interactions between the material constituents. Here, nonlinear continuum mechanics of an elastomer network is coupled to energetics of a nematic phase liquid crystal to quantify elastomer deformation due to the formation of liquid crystal domain structures.

The outline of the paper is given as follows. In Section 2, the governing equations for the liquid crystal elastomer are presented. Relations between the spatial and reference configurations are described to formulate free energy functions that lead to coupling between the liquid crystal molecular orientation (i.e., director) and the elastomer network. Similar techniques have been applied to dielectric elastomers [22–24]. Free energy functions are introduced to quantify mechanical energy of stretching an elastomer network and free energy that quantifies the formation and evolution of liquid crystal domains. In Section 3, the model is implemented using a finite element phase field method and formation of liquid crystal domains is presented. The case of a decoupled liquid crystal is compared to the fully coupled liquid crystal elastomer. Discussion is given in Section 4 and concluding remarks are given in Section 5.

[1]Email: hongbo@eng.fsu.edu, Tel: (850)410-6172
[2]Email: woates@eng.fsu.edu, Tel: (850) 410-6190

## 2. Governing Equations

In order to formulate the governing equations for a nematic phase liquid crystal elastomer, a free energy function is constructed. The function consists of the components per unit current volume

$$\psi = \psi_M(F_{iK}) + \psi_L(n_i, n_{i,j}) \tag{1}$$

where $\psi_M(F_{iK})$ is the free energy of the elastomer network and $F_{iK}$ is deformation gradient. The free energy of the liquid crystal is denoted by $\psi_L(n_i, n_{i,j})$ where $n_i$ is an order parameter defining orientation of the liquid crystal mesogen. The gradient on the liquid crystal is defined by $n_{i,j}$. Note that the liquid crystal director $n_i$ and its gradient $n_{i,j}$ are both defined in the spatial configuration. We assume that the free energy of the liquid crystal material and elastomer network is decoupled. This is an idealized case; however, it will illustrate how coupling appears between the elastomer network and director when finite deformation is considered.

Whereas the free energy of liquid crystal materials is decouled in the spatial configuration, coupling between the deformation gradient and liquid crystal director occurs when the energy is written in the reference configuration. This is illustrated by transforming the liquid crystal energy to the reference configuration

$$\tilde{\psi}_L = \tilde{\psi}_L(F_{iK}, \tilde{n}_K, \tilde{n}_{K,L}) \tag{2}$$

where $\tilde{n}_L$ and $\tilde{n}_{K,L}$ are the liquid crystal director and the gradient of a liquid crystal director in the reference configuration, respectively. The relationships of the director and its gradient in reference and spatial configurations are

$$\begin{aligned} n_i &= J^{-1} F_{iK} \tilde{n}_K \\ n_{i,j} &= J^{-1} F_{iK} F_{jL} \tilde{n}_{KL} \end{aligned} \tag{3}$$

The free energy function in the reference configuration is therefore denoted by

$$\tilde{\psi} = \tilde{\psi}_M(F_{iK}) + \tilde{\psi}_L(F_{iK}, \tilde{n}_K, \tilde{n}_{K,L}) \tag{4}$$

Apply the variational method to the free energy function in the reference configuration gives

$$\begin{aligned} \delta\tilde{\psi} &= \delta\tilde{\psi}_M(F_{iK}) + \delta\tilde{\psi}_L(F_{iK}, \tilde{n}_K, \tilde{n}_{K,L}) \\ &= \left(\frac{\partial\tilde{\psi}_M}{\partial F_{iK}} + \frac{\partial\tilde{\psi}_L}{\partial F_{iK}}\right)\delta F_{iK} + \left(\frac{\partial\tilde{\psi}_L}{\partial\tilde{n}_K}\right)\delta\tilde{n}_K + \left(\frac{\partial\tilde{\psi}_L}{\partial\tilde{n}_{K,L}}\right)\delta\tilde{n}_{K,L} \end{aligned} \tag{5}$$

and the total energy is given by integrating (5) over the reference volume $V_0$

$$\begin{aligned} \delta\tilde{\Psi} &= \int_{\Omega_0} \delta\tilde{\psi} dV_0 \\ &= \int_{\Omega_0} \left(\frac{\partial\tilde{\psi}_M}{\partial F_{iK}} + \frac{\partial\tilde{\psi}_L}{\partial F_{iK}}\right)\delta F_{iK} dV_0 + \int_{\Omega_0} \frac{\partial\tilde{\psi}_L}{\partial\tilde{n}_K}\delta\tilde{n}_K dV_0 + \int_{\Omega_0} \frac{\partial\tilde{\psi}_L}{\partial\tilde{n}_{K,L}}\delta\tilde{n}_{K,L} dV_0 \end{aligned} \tag{6}$$

Use divergence theorem on the first and third terms in (6) results in a set of governing equations

$$\begin{aligned} \frac{\partial(s_{iK} + s^L_{iK})}{\partial X_K} &= 0 \\ \frac{\partial\tilde{\xi}_{KL}}{\partial X_K} - \tilde{\eta}_L &= 0 \end{aligned} \tag{7}$$

in the reference volume subjected to a set of boundary conditions [25]. Here, $s_{iK}$ is the nominal stress of the elastomer network and $s^L_{iK}$ is the nominal stress contributed by liquid crystal materials. $\tilde{\xi}_{KL}$ and $\tilde{\eta}_L$ are the micro-stress and effective liquid crystal molecular field, respectively. They are defined as

$$s_{iK} = \frac{\partial \tilde{\psi}_M}{\partial F_{iK}}, \qquad s^L_{iK} = \frac{\partial \tilde{\psi}^L_M}{\partial F_{iK}}$$
$$\begin{aligned} \tilde{\xi}_{KM} &= \frac{\partial \tilde{\psi}_L}{\partial \tilde{n}_{K,M}} \\ \tilde{\eta}_K &= \frac{\partial \tilde{\psi}_L}{\partial \tilde{n}_K} \end{aligned} \tag{8}$$

The nominal stresses, effective molecular field, and micro-stress tesnor are related through the reference and spatial configurations by

$$\begin{aligned} \sigma_{ij} + \sigma^L_{ij} &= J^{-1} F_{jK}(s_{iK} + s^L_{iK}) \\ \eta_i &= H_{iK}\tilde{\eta}_K \\ \xi_{ij} &= H_{iK}H_{jL}\tilde{\xi}_{KL} \end{aligned} \tag{9}$$

where $H_{iK}$ is the inverse deformation gradient which has the properties, $H_{iK}F_{jK} = \delta_{ij}$ and $H_{iK}F_{iL} = \delta_{KL}$ where $\delta_{ij}$ and $\delta_{KL}$ are the Kronecker deltas [26].

The free energy of liquid crystal materials is comprised of two parts. The Landau liquid crystal energy and Frank elastic energy. In subsections 2.1 and 2.2, phenomenological energy functions for different components of the liquid crystal energy are introduced and used to quantify fields and stresses in the reference and spatial configurations. In subsection 2.3, mechanical energy will be introduced.

## 2.1 Landau liquid crystal energy

The Landau energy component for the liquid crystal energy is defined by a truncated polynomial with second and fourth order components. In the spatial configuration, the Landau energy is

$$\psi_{La}(n_i) = \frac{a_{ij}}{2} n_i n_j + \frac{b_{ijst}}{4} n_i n_j n_s n_t \tag{10}$$

where $a_{ij}$ and $b_{ijst}$ are phenomenological constants that define the liquid crystal phase characteristics. These terms are often temperature dependent. In this paper, the coefficients are assumed under isothermal conditions at temperatures below the isotropic-to-nematic transition point. These coefficients are also considered to be independent of the deformation gradient. The effective molecular field in the spatial configuration is

$$\eta_i = \frac{\partial \psi}{\partial n_i} = a_{ij} n_j + b_{ijst} n_j n_s n_t \tag{11}$$

Using $(3)_1$ and (10), the Landau energy is rewritten in the reference configuration

$$\tilde{\psi}_{La}(F_{iK}, \tilde{n}_K) = \frac{a_{ij}}{2} J^{-1} F_{iK}F_{jL}\tilde{n}_K\tilde{n}_L + \frac{b_{ijst}}{4} J^{-3} F_{iK}F_{jL}F_{sM}F_{tN}\tilde{n}_K\tilde{n}_L\tilde{n}_M\tilde{n}_N \tag{12}$$

which gives an effective molecular field in the reference configuration

$$\tilde{\eta}_K = \frac{\partial \tilde{\psi}_{La}}{\partial n_K} = a_{ij} J^{-1} F_{iK}F_{jL}\tilde{n}_L + b_{ijst} J^{-3} F_{iK}F_{jL}F_{sM}F_{tN}\tilde{n}_L\tilde{n}_M\tilde{n}_N. \tag{13}$$

The energy given by (12) has been defined such that the field in (13) is consistent with the spatial field relation given by (11). Consistency between the two fields can be shown by pre-multiplication of (13) by the inverse deformation gradient $H_{rK}$

$$H_{rK}\tilde{\eta}_K = a_{ij} J^{-1} H_{rK}F_{iK}F_{jL}\tilde{n}_L + b_{ijst} J^{-3} H_{rK}F_{iK}F_{jL}F_{sM}F_{tN}\tilde{n}_L\tilde{n}_M\tilde{n}_N \tag{14}$$

which reduces to (11) by substitution of $(3)_1$.

The mechanical coupling between the liquid crystal director and elastomer network is obtained by calculating the nominal stress relation from the energy function (12) according to

$$s_{iK}^{L(La)} = \frac{\partial \tilde{\psi}_{La}}{\partial F_{iK}} \tag{15}$$

which gives

$$\begin{aligned} s_{rM}^{L(La)} &= a_{rj}J^{-1}F_{jL}\tilde{n}_M\tilde{n}_L - \frac{a_{ij}}{2}J^{-1}H_{rM}F_{iK}F_{jL}\tilde{n}_K\tilde{n}_L + b_{rjst}J^{-3}F_{jL}F_{sP}F_{tQ}\tilde{n}_M\tilde{n}_L\tilde{n}_P\tilde{n}_Q\ldots \\ &\quad -\frac{3b_{ijst}}{4}J^{-3}H_{rM}F_{jL}F_{iK}F_{sP}F_{tQ}\tilde{n}_K\tilde{n}_L\tilde{n}_P\tilde{n}_Q \end{aligned} \tag{16}$$

where the relation $\dfrac{\partial J}{\partial F_{iK}} = JH_{iK}$ has been applied; see [25]. By application of equation $(9)_1$ for the liquid crystal stress component, the stress due to the Landau energy is

$$\begin{aligned} \sigma_{rn}^{L(La)} &= a_{rj}n_jn_n - \frac{a_{ij}}{2}n_in_j\delta_{rn} + b_{rjst}n_jn_sn_tn_n\ldots \\ &\quad -\frac{3}{4}b_{ijst}n_in_jn_sn_t\delta_{rn} \end{aligned} \tag{17}$$

and in the simplified case where $a_{ij} = a_0\delta_{ij}$ and $b_{ijst} = b_0\delta_{ij}\delta_{st}$, this liquid crystal stress reduces to

$$\begin{aligned} \sigma_{rn}^{L(La)} &= a_0n_rn_n - \frac{a_0}{2}n_jn_j\delta_{rn} + b_0n_rn_tn_tn_n\ldots \\ &\quad -\frac{3}{4}b_0n_jn_jn_tn_t\delta_{rn} \end{aligned} \tag{18}$$

which is often sufficient to describe nematic phase liquid crystal behavior by restricting $a_0 < 0$.

## 2.2 Frank elastic energy

Liquid crystals often form into polydomain structures containing several regions of uniform director orientation separated by domain walls. During deformation, the internal liquid crystal structure may evolve from a monodomain to a polydomain state which depends on the stress, loading rate, liquid crystal phase, elastomer network, etc. Frank elastic energy is introduced in this section to accommodate such domain structure evolution. Coupling to the Cauchy stress is presented here using similar arguments as presented in Section 2.1.

A generalized energy function for the Frank elastic energy is defined by

$$\psi_{Fr}(n_{i,j}) = \frac{a_{ijst}}{2}n_{i,j}n_{s,t} \tag{19}$$

in the spatial domain. The micro-stress tensor is

$$\xi_{ij} = \frac{\partial \psi}{\partial n_{i,j}} = a_{ijst}n_{s,t} \tag{20}$$

Note that this tensor includes both symmetric and anti-symmetric terms, $\xi_{ij} = \xi_{ij}^s + \xi_{ij}^a$.

A self-consistent energy relation can be written in the reference domain to illustrate coupling between the director gradient and stress. The Frank elastic energy in the reference domain is

$$\tilde{\psi}_{Fr}(F_{iK}, \tilde{n}_{K,L}) = a_{ijst}J^{-1}F_{iK}F_{jL}F_{sM}F_{tN}\tilde{n}_{K,L}\tilde{n}_{M,N} \tag{21}$$

The gradient field based on the reference description is given by

$$\tilde{\xi}_{KL} = \frac{\partial \tilde{\psi}}{\partial \tilde{n}_{K,L}} = a_{ijst}J^{-1}F_{iK}F_{jL}F_{sM}F_{tN}\tilde{n}_{M,N} \tag{22}$$

which reduces to (20) by substitution of $(3)_2$ and $(9)_3$ into (22).

The stress due to a polydomain configuration is obtained similar to the monodomain liquid crystal stress by first introducing the nominal stress component. In this case, the nominal stress component due to polydomain structures is

$$\begin{aligned} s_{rP}^{L(Fr)} &= \frac{\partial \tilde{\psi}_{Fr}}{\partial F_{rP}} \\ &= 2a_{rjst}J^{-1}F_{jL}F_{sM}F_{tN}\tilde{n}_{P,L}\tilde{n}_{M,N} - \frac{a_{ijst}}{2}F_{iK}F_{jL}F_{sM}F_{tN}\tilde{n}_{K,L}\tilde{n}_{M,N}H_{rP} \end{aligned} \tag{23}$$

and the Cauchy liquid crystal stress component is

$$\sigma_{qr}^{L(Fr)} = 2a_{rjst}n_{q,j}n_{s,t} - \frac{a_{ijst}}{2}n_{i,j}n_{s,t}\delta_{rq} \tag{24}$$

The generalized energy relation defined in (19) and liquid crystal stresses can be simplified using the typical Frank elastic energy given in the literature in terms of three phenomenological parameters [27, 28]. This energy function is

$$\psi_{Fr}(n_{i,j}) = \frac{1}{2}K_1\left(n_{i,i}n_{j,j}\right) + \frac{1}{2}K_2\left(\in_{pjk}\in_{pst} n_p n_q n_{k,j} n_{t,s}\right) + \frac{1}{2}K_3\left(\in_{pmi}\in_{pjk}\in_{qmr}\in_{qst} n_i n_{k,j} n_r n_{t,s}\right) \tag{25}$$

where the first term penalizes splay, the second term penalizes twist, and the third term penalizes bending of the liquid crystal director. In the single constant approximation, this energy reduces to

$$\psi_{Fr}(n_{i,j}) = \frac{1}{2}K n_{i,j}n_{i,j} \tag{26}$$

and using the single constant approximation, the fourth order tensor $a_{ijkl}$ is related to $K$ by

$$a_{ijkl} = K\delta_{ik}\delta_{jl} \tag{27}$$

The distortional stress is found to be symmetric in the single constant approximation by substitution of (27) into (24). This allows conventional elastic energy functions to be used to construct mechanical energy functions for stretching an elastomer network in the presence of liquid crystals without violating angular momentum relations. This single constant approximation will be used for numerical implementation in combination with an isotropic elastic energy function given in the following section.

## 2.3 Mechanical energy

To simplify the problem, an isotropic energy function is introduced for numerical implementation of the liquid crystal elastomer model. The elastic energy function is

$$\tilde{\psi}_M(E_{IJ}) = \frac{1}{2}c_{ijkl}E_{IJ}E_{KL} \tag{28}$$

where $c_{ijkl}$ is the fourth order elasticity tensor. The Green-Lagrange finite strain tensor has been introduced as

$$E_{IJ} = \frac{1}{2}\left(\frac{\partial u_i}{\partial X_J} + \frac{\partial u_j}{\partial X_I} + \frac{\partial u_k}{\partial X_I}\frac{\partial u_k}{\partial X_J}\right) \tag{29}$$

where $u_i(X_K) = x_i(X_K) - X_I$ and the displacement gradient is related to the deformation gradient by $\dfrac{\partial u_i}{\partial X_J} = F_{iJ} - \delta_{iJ}$ where $\delta_{iJ}$ is the Kronecker delta.

The second Piola-Kirchoff stress $\tilde{T}_{IJ}$, which is conjugate to the finite strain tensor, can be implemented to accommodate large deformation [25, 26]

$$\tilde{T}_{IJ} = c_{ijkl}E_{KL} \tag{30}$$

Also note that the Cauchy stress due to the elastomer is related to the second Piola-Kirchoff stress by the relation

$$\sigma_{ij} = J^{-1} F_{iK} F_{jL} \tilde{T}_{KL} \tag{31}$$

An isotropic elastic tensor is introduced in the following section to illustrate liquid crystal behavior within an elastomer. For convenience, the elastic tensor is written in terms of the shear and bulk modulus as

$$c_{ijkl} = \left( K_M - \frac{2}{3}\mu \right) \delta_{ij}\delta_{kl} + \mu(\delta_{ik}\delta_{jl} + \delta_{il}\delta_{jk}) \tag{32}$$

where $K_M$ is the bulk modulus and $\mu$ is the shear modulus. Whereas more accurate hyperelastic energy functions could be introduced using this modeling framework, first order elasticity effects are condsidered here. Therefore, the elasticity coefficients are assumed to be independent of the deformation in the numerical model given in the following section.

# 3. Numerical Implementation

A nonlinear finite element approach is applied here to implement the liquid crystal elastomer model. The weak form of the governing equations (7) are

$$\begin{aligned} \int_{\Omega_0} w_{i,J}(s_{iJ} + s^L_{iJ}) dV_0 &= \int_{\Gamma_0} w_i (s_{iJ} + s^L_{iJ}) \hat{N}_J dS_0 \\ \int_{\Omega_0} \left( w_{I,J} \tilde{\xi}_{JI} + w_I \tilde{\eta}_I \right) dV_0 &= \int_{\Gamma_0} w_I \tilde{\xi}_{JI} \hat{N}_J dS_0 \end{aligned} \tag{33}$$

where the weight function for mechanical equilibrium is $w_i$ and the weight function for the liquid crystal configurational force balance is denoted by $w_I$. A unit normal in the reference configuration has been denoted by $\hat{N}_J$.

The elastic nominal stress determined from the second order Piola-Kirchoff stress and constitutive relation

$$s^M_{iJ} = J^{-1} F_{iI} \tilde{T}^M_{IJ} = J^{-1} F_{iI} c_{IJKL} E_{KL} \tag{34}$$

where upper case indicial notation has been used for the elastic tensor $c_{IJKL}$. The additional nominal stress terms due to liquid crystal structure are calculated based on (16) and (23). The equilibrium domain structure under zero traction is of interests here; therefore, the infinitesimal strain assumption is used. This simplifies the numerical implementation of the model by neglecting higher order deformation gradient components. However, the model does include liquid crystal coupling in the Cauchy stress. The same approximation is applied when the micro-stress (22) and effective molecular field (13) are numerically implemented.

A summary of the parameters used in our model are listed in the Table 1.

Table 1: Parameters used in the finite element liquid crystal phase field model.

| Name | Value | Unit |
|---|---|---|
| K | $7 \times 10^{-12}$ | N |
| $a_0$ | $-2 \times 10^5$ | $N/m^2$ |
| $b_0$ | $2 \times 10^5$ | $N/m^2$ |
| $K_M$ | $1 \times 10^7$ | $N/m^2$ |
| $\mu$ | $2 \times 10^6$ | $N/m^2$ |

A series of test simulations have been carried on by use of the parameters from Table 1. Our preliminary results predict very small strain (of the order $10^{-4}$) for the coupling between the liquid crystal and elastomer network. Therefore, approximation of the Green strain tensor as the infinitesimal strain tensor is justified. Under

this approximation, the nominal stress and Cauchy stress are equivalent. The nominal stresses contributed by Landau energy and distortional energy can be approximated by (18) and the expression

$$\sigma_{qr}^{L(Fr)} = 2Kn_{q,j}n_{r,j} - \frac{K}{2}n_{i,j}n_{i,j}\delta_{rq} \tag{35}$$

Accordingly the effective molecular field and the micro-stress tensor are calculated by

$$\begin{aligned} \tilde{\eta}_K &= a_0 n_K + b_0 n_K n_s n_s \\ \tilde{\xi}_{IJ} &= K n_{I,J} \end{aligned} \tag{36}$$

In our simulations, the initial conditions of the liquid crystal director is a small random perturbation with magnitude $\sim 1 \times 10^{-6}$. Two different cases will be considered and compared. In one case, a nematic phase liquid crystal and in the second case, a fully coupled nematic phase liquid crystal elastomer using the same liquid crystal energy and parameter values.

# 4. Results and Discussion

The liquid crystal elastomer was modeled using a $2 \times 2\mu m^2$ rectangle with traction and micro-stress free boundaries. The bottom left corner is fixed in the vertical and horizontal direction and the right bottom corner is fixed in the vertical direction. The finite element mesh and the initial condition are shown in Figure 1.

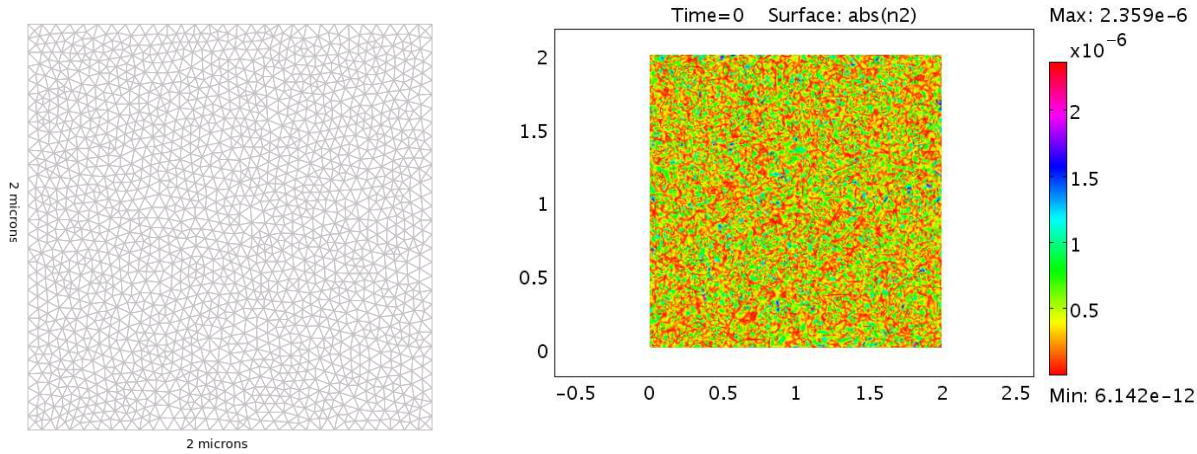


(a) (b)

Figure 1: (a) Mesh grid for both the decoupled and coupled simulation. The mesh consists of 3468 elements. The maximum mesh size is $70nm$. In (b) the initial condition is a random director with magnitude $|\mathbf{n}| = 1 \times 10^{-6}$.

Figures 2 and 3, compare the decoupled liquid crystal behavior at equilibrium to the liquid crystal elastomer domain structure (i.e., fully coupled case), respectively. From both the figures, it can be seen that typical domain structures with domain size on the order of microns form. Several point defects appear after starting from a small random director distribution, in which the director value is $|\mathbf{n}| < 1 \times 10^{-6}$. The use of the small strain approximation explains the similarity of the domain structures for both the coupled and decoupled cases since partial coupling of the director to the Cauchy stress occurs. Current work is focused on liquid crystal director reorientation under large deformation where explicit coupling to the director under large deformation will occur.

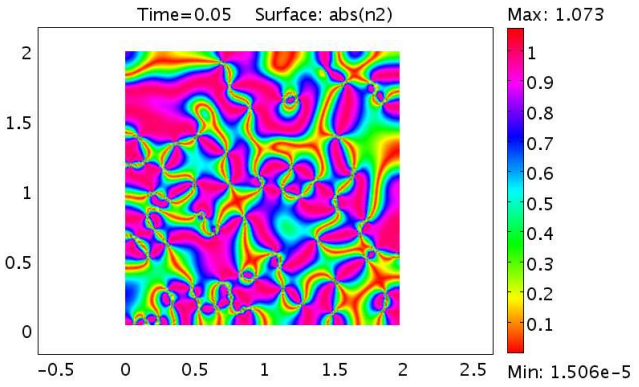


(a)

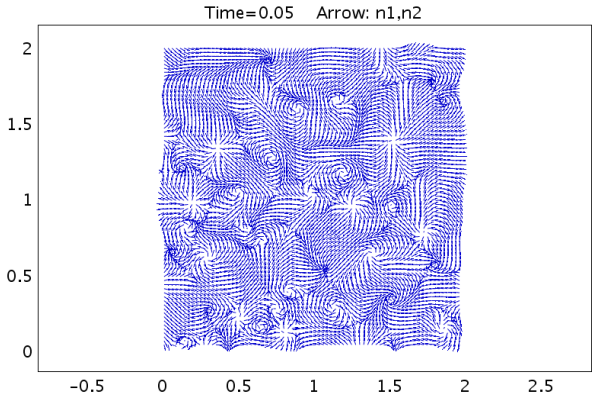


(b)

Figure 2: Equilibrium domain structures that formed for a liquid crystal in the decoupled case where finite deformation of the elastomer is not included in the governing equations. In (a), the director component in the vertical direction ($n_2$) is shown. In (b), the arrows representing the director orientation is given.

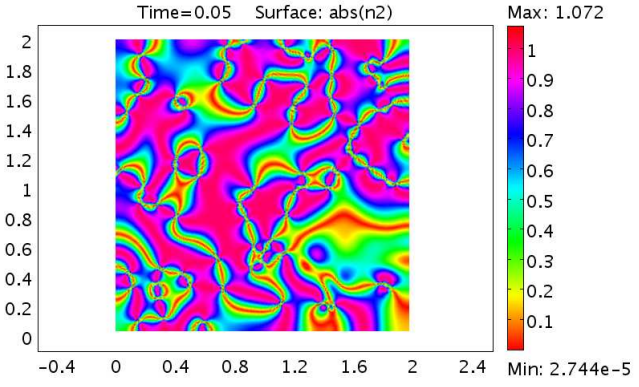


(a)

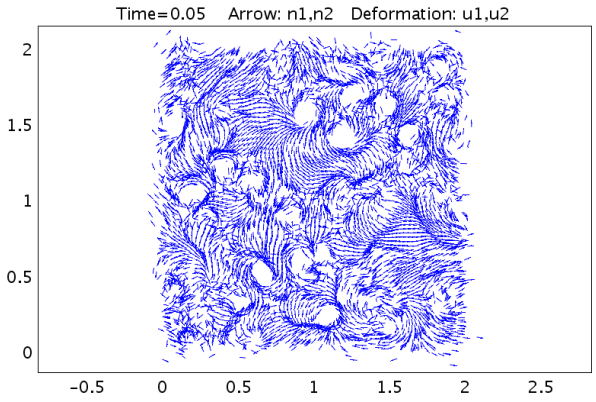


(b)

Figure 3: Equilibrium domain structure formation for the liquid crystal *elastomer*. Again in (a), the director component in the vertical direction ($n_2$) is shown. In (b), the arrows representing the director orientation is given.

# 5. Conclusion

A nonlinear phase field model for liquid crystal elastomer is presented in this paper. Field-coupled relations are established by introducing configurational liquid crystal forces with energetics of mechanical stretching an elastomer network. The model is numerically implementation to quantify domain structure formation. In the infinitesimal strain case, similar liquid crystal domain structures are predicted between the decoupled liquid crystal model and the coupled liquid crystal elastomer model. Our model provides important insight of liquid crystal structure evolution and coupling with an elastomer, which paves the road for future work in large

deformation applications, electro-mechanical coupling, and photoelastomer coupled behavior to understand how to exploit these materials in a variety of artificial muscle applications.

## Acknowledgments

Financial support was kindly provided by Center of Excellence, Florida Center for Advanced Aero-Propulsion-FCAAP.

## References

[1] J. Ericksen, *Arch. Ration. Mech. Analysis*, vol. 23, p. 266, 1966.

[2] E. Nishikawa and H. Finkelmann, "Smectic A liquid single crystal elastomers showing macroscopic in-plane fluidity," *Macromol. Rapid Commun.*, vol. 18, pp. 65–71, 1997.

[3] N. A$\beta$falg and H. Finkelmann, "A Smectic A liquid crystal elastomer (LSCE): Phase behavior and mechanical anisotropy," *Macromol. Chem. Phys.*, vol. 202, pp. 794–800, 2001.

[4] B. Donnio, H. Wermter, and H. Finkelmann, "A simple and versatile synthetic route for the preparation of main-chain, liquid crystal elastomers," *Macromolecules*, vol. 33, pp. 7724–7729, 2000.

[5] B. Acharya, A. Primak, and S. Kumar, "Biaxial nematic phase in bent-core thermotropic mesogens," *Phys. Rev. Lett.*, vol. 92, no. 14, pp. 145 506–1–145 506–4, 2004.

[6] W. Lehmann, H. Skupin, C. Tolksdorf, E. Gebhard, R. Zentel, P. Krüger, M. Lösche, and F. Kremer, "Giant lateral electrostriction in ferroelectric liquid-crystalline elastomers," *Nature*, vol. 410, pp. 447–450, 2001.

[7] C. Spillman, B. Ratna, and J. Naciri, "Anisotropic actuation in electroclinic liquid crystal elastomers," *Appl. Phys. Lett.*, vol. 90, pp. 021 911–1–021 911–3, 2007.

[8] J. Harden, B. Mbanga, N. Éber, K. Fodor-Csorba, S. Sprunt, J. Gleeson, and A. Jákli, "Giant flexoelectricity of bent-core nematic liquid crystals," *Liquid Crystal Communications*, pp. 1–11, 2006. [Online]. Available: http://www.e-lc.org/docs/2006_07_18_08_47_15

[9] T. Ikeda, J. Mamiya, and Y. Yu, "Photomechanics of liquid-crystalline elastomers and other polymers," *Angew. Chem.*, vol. 46, pp. 506–528, 2007.

[10] H. Koerner, T. White, N. Tabirya, T. Bunning, and R. Vaia, "Photogenerating work from polymers," *Materials Today*, vol. 11, no. 7–8, pp. 34–42, 2008.

[11] K. Harris, R. Cuypers, P. Scheibe, C. van Oosten, C. Bastiaansen, J. Lub, and D. Broer, "Large amplitude light-induced motion in high elastic modulus polymer actuators," *J. Mater. Chem.*, vol. 15, pp. 5043–5048, 2005.

[12] I. Rousseau and P. Mather, "Shape memory effect exhibited by smectic-C liquid crystalline elastomers," *J. Am. Chem. Soc.*, vol. 125, pp. 15 300–15 301, 2003.

[13] P. Martinoty, P. Stein, H. Finkelmann, H. Pleiner, and H. Brand, "Mechanical properties of monodomain side chain nematic elastomers," *Eur. Phys. J. E*, vol. 14, pp. 311–321, 2004.

[14] T. Lubensky, R. Mukhopadhyay, L. Radzihovsky, and X. Xing, "Symmetries and elasticity of nematic gels," *Phys. Rev. E*, vol. 66, pp. 011 702–1–011 702–22, 2002.

[15] E. Terentjev, M. Warner, and G. Verwey, "Non-uniform deformations in liquid crystalline elastomers," *J. Phys. II France*, vol. 6, pp. 1049–1060, 1996.

[16] E. Terentjev, "Phenomenological theory of non-uniform nematic elastomers: Free energy of deformations and electric-field effects," *Europhys. Lett.*, vol. 23, no. 1, pp. 27–32, 1993.

[17] M. Warner and S. Kutter, "Uniaxial and biaxial soft deformations of nematic elastomers," *Phys. Rev. E*, vol. 65, pp. 051 707–1–051 707–9, 2002.

[18] E. Fried and S. Sellers, "Free-energy density functions for nematic elastomers," *J. Mech. Phys. Solids*, vol. 52, pp. 1671–1689, 2004.

[19] J. Adams, S. Conti, and A. DeSimone, "Soft elasticity and microstructure in smectic C elastomers," *Continuum Mech. Thermodyn.*, vol. 18, pp. 319–334, 2007.

[20] J. Adams and M. Warner, "Elasticity of smectic-A elastomers," *Phys. Rev. E*, vol. 71, pp. 021 708–1–021 708–15, 2005.

[21] S. Conti, A. DeSimone, and G. Dolzmann, "Soft elastic response of stretched sheets of nematic elastomers: a numerical study," *J. Mech. Phys. Solids*, vol. 50, pp. 1431–1451, 2002.

[22] G. Kofod and P. Sommer-Larsen, "Silicone dielectric elastomer actuators: Finite-elasticity model of actuation," *Sensors and Actuators A*, vol. 122, pp. 273–283, 2005.

[23] R. McMeeking and C. Landis, "Electrostatic forces and stored energy for deformable dielectric materials," *J. Appl. Mech*, vol. 72, pp. 581–590, 2005.

[24] X. Zhao, W. Hong, and Z. Suo, "Electromechanical hysteresis and coexistent states in dielectric elastomers," *Phys. Rev. B*, vol. 76, pp. 134 113–1–134 113–9, 2007.

[25] G. Holzapfel, *Nonlinear Solid Mechanics*. Chichester: John Wiley & Sons, Inc., 2000.

[26] L. Malvern, *Introduction to the Mechanics of a Continuous Medium*. Englewood Cliffs, NJ: Prentice-Hall, Inc., 1969.

[27] P. de Gennes and J. Prost, *The Physics of Liquid Crystals*. Oxford: Oxford Science Publications, 1993.

[28] M. Warner and E. Terentjev, *Liquid Crystal Elastomers–Revised Edition*. Oxford: Oxford Science Publications, 2007.